NASA
Technical Memorandum 4146

AVSCOM
Technical Memorandum 89-B-009

Effect of Blade Planform Variation on a Small-Scale Hovering Rotor

Susan L. Althoff and Kevin W. Noonan

JANUARY 1990

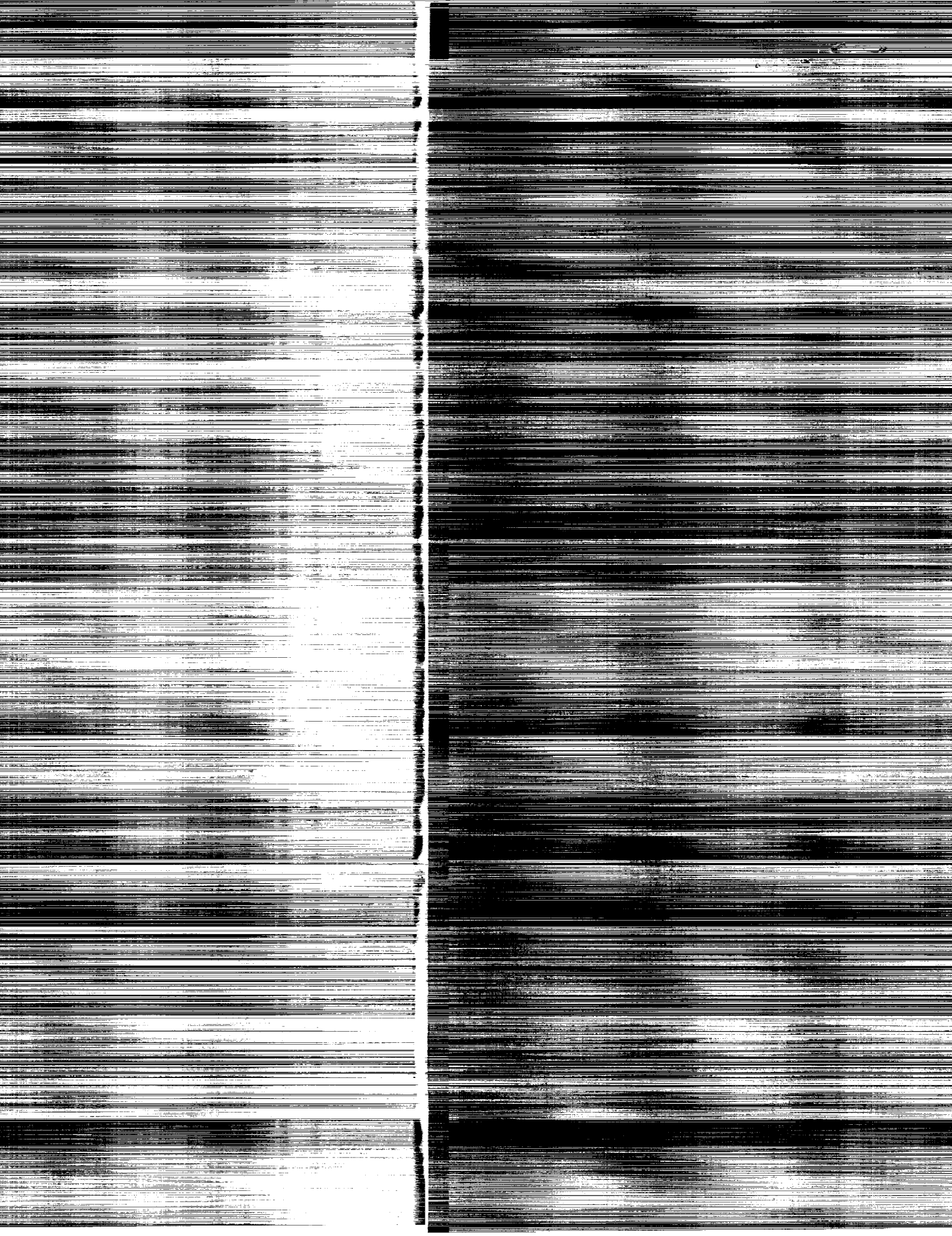

NASA
Technical Memorandum 4146

AVSCOM
Technical Memorandum 89-B-009

Effect of Blade Planform Variation on a Small-Scale Hovering Rotor

Susan L. Althoff and Kevin W. Noonan
Aerostructures Directorate
USAARTA-AVSCOM
Langley Research Center
Hampton, Virginia

National Aeronautics and
Space Administration
Office of Management
Scientific and Technical
Information Division

1990

Summary

A hover test was conducted on a small-scale rotor model for three sets of tapered rotor blades and a baseline rectangular-planform rotor blade. All configurations had the same airfoils, twist, and thrust-weighted solidity. The tapered-blade planforms had taper initiating at 50, 75, and 94 percent of the blade radius with a taper ratio of 3 to 1 for each blade set. The experiment was conducted for a range of thrust coefficients, and the data were compared with the predictions of three hover analytical methods. The data show that the 94-percent tapered blade was slightly more efficient at the higher rotor thrust levels. The other tapered-planform rotors did not show the expected improvement over the baseline rotor, and all configurations had a similar performance for low thrust coefficients. None of the analytical methods correlated well with the experimental data.

Introduction

Many studies have been conducted to determine the optimum rotor-blade tip shape to increase both hover and forward flight performance, as well as to reduce rotor noise. Typical tip shapes that have been investigated are rectangular, trapezoidal, tapered, swept-tapered, and ogee. (See, for example, refs. 1–9.) The U.S. Army Aerostructures Directorate at the NASA Langley Research Center has been investigating the performance of tapered rotor blades for several years (refs. 10–13). The purpose of the present investigation was to isolate the effect of the radial position of taper initiation on the hovering performance of a rotor.

A hover study has been conducted using three tapered rotor systems and a baseline rectangular rotor system. The tapered-blade planforms had taper initiating at 50, 75, and 94 percent of the blade radius with a taper ratio of 3 to 1 for each blade set. The 75-percent taper-initiation planform was an existing rotor set, and the 50-percent taper-initiation planform was chosen as the most inboard location based on the experimental results in reference 11. The position of the 94-percent taper initiation was chosen based on analytical predictions of improvements in forward flight performance with taper initiation in the blade tip region. The rotors had identical twist and thrust-weighted solidity, and they were tested over a range of thrust coefficients. The experimental data were compared with the hover performance predictions of three analytical methods. One of the methods used a momentum blade-element analysis, whereas the other two methods used a free-wake lifting-surface method.

Symbols

The data in this report were measured in U.S. Customary Units and are referenced to the shaft axis system shown in figure 1.

C_Q	rotor torque coefficient, $M_Z/\rho\pi R^3(\Omega R)^2$
C_T	rotor thrust coefficient, $T/\rho\pi R^2(\Omega R)^2$
D	rotor drag force, lbf
FM	rotor figure of merit, $C_T^{3/2}/C_Q\sqrt{2}$
L	rotor lift force, lbf
M_Z	rotor torque, ft-lbf
R	rotor radius, ft
r	radial distance along blade, ft
T	rotor thrust, $(L^2 + D^2 + Y^2)^{1/2}$, lbf
x, y, z	Cartesian coordinates (see fig. 1)
Y	rotor side force, lbf
ρ	atmospheric density of air, slugs/ft^3
Ω	rotor rotational speed, rad/sec

Abbreviations and acronyms:

HOVER	lifting-surface hover-performance code
LSAF	Lifting-Surface Aerodynamics and Performance Analysis of Rotors in Axial Flight
RGMX	position of maximum circulation input into HOVER analysis
ROBIN	generic fuselage shell
RTC	rotor test cell
2MRTS	2-meter rotor test system

Model and Test Description

The test program was conducted in the rotor test cell (RTC) at the Langley 14- by 22-Foot Subsonic Tunnel. The RTC is a high-bay area that is 69 ft high by 42 ft wide by 48 ft long with a steel chain link fence around the walls; it is arranged specifically for the buildup and testing of powered rotor models in hover. Two walls of the RTC have louvers that can be opened to alleviate some of the recirculation of air from the hovering rotor. The density was measured locally in the RTC. The rotor hub was located 1.74 rotor diameters above the floor of the RTC on a post mount. The model is pictured mounted for testing in the RTC in figure 2.

The model system used for this experiment was the 2-meter rotor test system (2MRTS) with a

generic fuselage shell (ROBIN). The ROBIN fuselage shape is described in reference 14. The 2MRTS is documented in reference 15, and only a brief description will be given here.

The 2MRTS is a drive system that consists of a 29-hp electric motor, a 90° two-stage transmission with a 4-to-1 gear reduction ratio, and a four-bladed rotor hub. (See fig. 2.) The hub is fully articulated with coincident flap and lag hinges.

Forces and moments are measured separately on the rotor and fuselage by two six-component, strain gauge balances. Other instrumentation of the system includes three strain gauges on the rotor blades to measure bending moments, potentiometers to measure flapping and lead-lag motion, a digital rotational speed (rpm) encoder, and thermocouples to monitor critical temperatures.

The four blade sets used in this investigation are shown in figure 3. As mentioned before, three of the blade sets had a tapered planform, whereas the fourth blade set was a baseline rectangular-planform rotor. The taper ratio for each set of tapered blades was 3 to 1; the difference among the blades was the radial position of the start of the taper. The position of the initiation of the taper was 50 percent radius for the first blade set, 75 percent radius for the second blade set, and 94 percent radius for the third blade set. All four blades had a 2.708-ft radius, −13° of linear twist, and a thrust-weighted solidity of 0.0977, and they used advanced rotorcraft airfoil sections.

The airfoil sections were developed by researchers of the U.S. Army Aerostructures Directorate at the NASA Langley Research Center specifically for rotorcraft applications. The airfoils used for this investigation were the advanced rotorcraft airfoils RC(4)-10, RC(3)-10, and RC(3)-08. In the RC(x)-xx format, the "RC" designates a rotorcraft airfoil, the "(x)" indicates the sequential number, and the "-xx" provides the thickness in percent of chord. The RC(3)-10 and RC(3)-08 airfoils are documented in reference 16. They were shown to have high drag-divergence Mach numbers and low pitching moments, but average high-lift characteristics. The RC(4)-10 airfoil (ref. 17) proved to have good high-lift capability, but the two-dimensional wind-tunnel test results have not been published at this time. The radial distribution of the airfoils along each rotor-blade set is shown in figure 3. The airfoil profiles are shown in sketch A and the coordinates are given in tables I–III for each of the airfoils.

The rotor blades were constructed using a graphite-epoxy D-spar with tungsten leading-edge weights and a balsa wood trailing edge. All the blade sets were very stiff as there was no attempt to match the aeroelastic characteristics of full-scale rotor blades. Smooth transitions were accomplished between the different airfoil sections over 5 percent of the blade radius.

The test procedure was as follows: the rotor rpm was established, a collective blade angle was input, and the shaft angle was set to zero. The flapping of the rotor blades was monitored and was maintained less than 0.01°. After the data had been collected for a given condition, the collective angle was increased and the procedure was repeated. The upper limit of the thrust sweep was determined by the motor power and temperature limits. Thrust sweeps were made at 2500 rpm for a range of thrust coefficients C_T from 0 to approximately 0.010 for each set of rotor blades.

The data were acquired through a static data acquisition system that sampled the data. Four hundred data measurements were acquired in 8 sec for each data point presented. Each thrust sweep was repeated in order that some measure of the data accuracy and scatter could be determined. One condition was tested on two different days in order to ensure that daily variances in temperature, humidity, and pressure were being properly corrected. The ambient winds in the RTC were measured daily, and data were acquired only when the wind conditions were less than 1 knot. The precision of the data measurements is estimated from the repeatability tests to be $\pm 7.3 \times 10^{-5}$ in thrust coefficient C_T and $\pm 5.0 \times 10^{-6}$

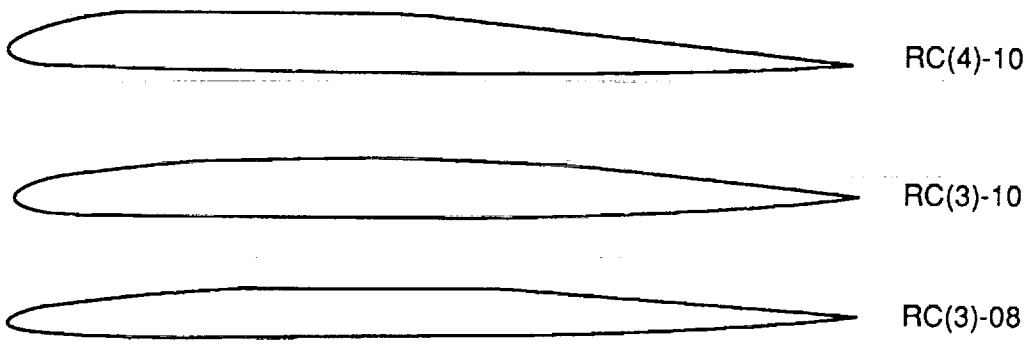

Sketch A

in torque coefficient C_Q. The uncertainty in rotor figure of merit (FM) is calculated by the method of reference 18 to be ± 0.011.

Description of Analytical Methods

The selection of the hover analytical methods used for this investigation was based on the experience with hover-performance codes in references 19 and 20. It was found in reference 20 that a simple momentum blade-element theoretical analysis and a lifting-surface method were capable of predicting the trend in hover performance due to advanced airfoils, whereas a second lifting-surface method was unable to converge to a solution for the tapered rotor blades used for that study. However, since that study was conducted, the second lifting-surface method has undergone several improvements. Therefore, it was decided to use these three analyses again to assess their ability to predict the effect of planform variation.

The momentum blade-element analysis used for this investigation is a code based on the equations developed in reference 21. The rotor disk is treated as an actuator disk consisting of concentric annular rings. Expressions for the differential thrust on each ring are obtained from both momentum and blade-element theories. Equating these expressions leads to a general equation for the induced velocity that varies with local chord and twist. The induced velocity is used to obtain the local angle of attack and Mach number. The blade air loads are obtained from two-dimensional airfoil tables. The total rotor forces and torque are determined by integrating the segment forces over the rotor blade.

The second analytical method used in this investigation was the lifting-surface hover-performance code (HOVER), which is documented in reference 22. The rotor blades are modeled using a vortex-lattice panel distribution, whereas the wake is represented by discrete vortex segments. The rotor wake geometry is determined through iteration. The first iteration consists of establishing a wake geometry from a set of prescribed-wake equations and matching the circulation solution of the rotor blades. In the second iteration, the rotor wake is allowed to distort as a free wake from the generalized wake solution in response to the induced velocities from the rotor blades and from self-induced velocities in the wake itself. After a wake geometry has been determined, HOVER calculates the circulation induced by the wake at the rotor-blade surface through use of the Biot-Savart law. Once the circulation is known, the lift can be calculated from the Kutta-Joukowski law. The drag is calculated by combining the induced drag with the airfoil profile drag from two-dimensional airfoil data. The rotor torque is calculated from the integrated rotor-blade drag. There is no model for airfoil stall or separation in HOVER. Compressibility effects on lift are calculated using a Prandtl-Glauert correction, whereas the effects on drag are assumed to be contained in the two-dimensional-airfoil data tables.

The third analytical method used in this investigation was the Lifting-Surface Aerodynamics and Performance Analysis of Rotors in Axial Flight (LSAF), which is discussed in references 23 and 24. The rotor blades and wake were represented as vortex boxes or lattices. The version of LSAF that was used for this study incorporated a velocity-coupled wake model into the program in addition to the prescribed wake model discussed in reference 24. It was shown in reference 20 that LSAF had difficulty converging to a solution. However, since that time the program has been upgraded, and this newer version of the program (version 1.08) incorporated changes to improve the convergence of the solution to a requested rotor thrust value. The calculations for the rotor performance are similar to those used in HOVER; i.e., the lift and induced drag are calculated using the circulation distribution, and the profile drag and torque calculations rely on two-dimensional airfoil data.

Presentation of Results

The experimental data are presented in tabular and graphical format. The values of thrust coefficient C_T, torque coefficient C_Q, and figure of merit FM for the baseline (rectangular) and tapered rotor blades can be found in tables IV–VII. The analytical comparisons to the experimental data are shown graphically. The presentations are made using the following figures:

Results and Discussion

Experimental Results

The results of the experiment are shown in figure 4 as plots of figure of merit and torque coefficient versus thrust coefficient. The data are also presented in tables IV–VII. Figure of merit is a rotor

efficiency term that expresses the ratio of the ideal power required for hover to the actual power required for hover.

Figure 4 shows that the data for the four rotor blades were very similar at thrust coefficients below 0.005. However, for the higher thrust coefficients, the 94-percent tapered blade appeared to have an advantage in efficiency. The data show that the 94-percent tapered blade produced approximately 6 percent greater FM at $C_T = 0.008$. Surprisingly, there were essentially no differences in the data for the 75-percent and 50-percent tapered planforms. They exhibited the same characteristics as the baseline rectangular blade until $C_T = 0.0088$, at which point the tapered planforms experienced a decrease in FM. All the rotor blades produced a maximum FM over a range of C_T from 0.0068 to 0.0088. This flat maximum region on the FM curve was similar to that seen in the data in reference 20, which was attributed to the characteristics of the advanced rotorcraft airfoil sections. Torque coefficient is also plotted against C_T in figure 4 for the four blade planforms to provide an indication of the power required by the rotor for the different configurations.

The data in figure 4 show trends in hover performance that were unexpected based on other experimental data in references 11 and 19. In those studies, the tapered-planform rotors showed improved performance over the baseline rotors, especially at low thrust coefficients. However, the comparison between these data and those in references 11 and 19 cannot be made directly because of the differences in the configurations of the tapered-planform rotors. In reference 11, the two-bladed tapered-planform rotor had a 2-to-1 taper ratio initiating at 50 percent radius and $-14°$ of linear twist. The four-bladed tapered rotors in reference 19 had 3-to-1 and 5-to-1 taper ratios initiating at 80 percent radius; the rotors had $-16°$ of linear twist and used an NACA 0012 airfoil section. Despite these differences, some improvement over the baseline blade was expected from all the tapered rotors used in the present investigation.

However, in reference 25, a parametric study was conducted for a hovering rotor that included tapered-planform effects. In that study, the number of blades was varied for an untwisted 0012 rotor with a 2-to-1 taper-ratio planform. It was shown that the greatest improvement in performance due to taper occurred on the two-bladed rotor. The improvement decreased as the number of blades increased from two to four. Since the present investigation used a four-bladed rotor system, the performance of the tapered-planform rotors was probably adversely affected.

It was initially thought that the difference in twist between the rotors of this test and those in references 11 and 19 might have been the reason that the tapered rotors in this test showed little difference from the baseline rotor. An attempt to assess the effect of twist on the rotor performance analytically was conducted and is discussed in the next section.

In order for all tapered rotor-blade sets to have the same thrust-weighted solidity, the inboard and tip chords of the blades had to vary. This variation produced a change in the tip Reynolds number among the blades since the blades were all tested at the same rotor tip speed. To investigate the effect of the varying tip Reynolds number, the tapered rotors were also tested at rotor tip speeds that generated approximately the same tip Reynolds number for each blade set (332 562). The rectangular blades were not tested at a reduced tip speed because the fiberglass skin on one of the blades delaminated after the full tip speed runs. It was shown in reference 20 that for the rotor blades with advanced rotorcraft airfoils, changing the tip Mach number produced little change in the performance of the rotor. The results are shown in figure 5 for the three tapered blades. There was very little change in the performance characteristics from those that were shown in figure 4, an indication that the variation in tip Reynolds number among the three tapered rotors had little effect on the performance data.

Analytical Results

The prediction of performance by analytical methods can be used for several different purposes. For example, a rotor designer needs an analysis that will predict the correct trends in performance for a systematic parametric study. Another use for the analyses is to predict the level of performance that would be expected for a given rotor. Figure 6 shows the ability of several analytical methods to predict performance trends, whereas figure 7 compares the ability of the analytical methods to predict performance levels. In all cases, a tension spline was applied to the analytical predictions to produce the curves shown in the figures, and airfoil data obtained at full-scale Reynolds numbers were used to make the predictions.

Figure 6 shows the predictions of the three analytical methods for the four rotor-blade configurations. None of the analyses predict the trend that was seen in the experimental data where there was little difference in the performance over most of the thrust range. The momentum method, and HOVER method as well, predict an increase in FM for all the tapered configurations over the baseline rectangular blade. The LSAF method predicts that the rectangular planform will have the highest efficiency, which does not agree with either the experimental data or

the other two analytical programs. It is clear from figure 6(c) that LSAF, despite the improvements to the program, is not able to converge to a steady-wake solution for the tapered-blade configurations. The LSAF predictions appear to worsen with the amount of taper of the configuration.

A comparison of the experimental data with the prediction methods is shown in figure 7. The momentum analytical method consistently predicted higher-than-measured efficiency. It may have predicted greater FM than the experimental data because full-scale Reynolds number airfoil data were used in the prediction. However, if the airfoil data were the only cause of the high prediction by the momentum method, the trends shown in figure 6(a) would have been correct. Both LSAF and HOVER made use of vortex wake models to compute rotor inflow. The solution depended heavily on an accurate wake-geometry representation. The LSAF predictions clearly reflected an inconsistently or insufficiently converged wake-geometry solution, thus leading to the highly nonlinear variation in FM with C_T. The HOVER solution also showed some slight nonlinearity in the FM versus C_T prediction.

The HOVER analytical predictions match the experimental data most closely for the 75-percent tapered rotor. For the other configurations, HOVER predicts less-than-measured performance. It is known from a previous study (ref. 20) that the HOVER predictions can be changed significantly by the user's choice of input, especially in the selection of the position of maximum circulation (RGMX). In the present study, no attempt was made to manipulate the HOVER output to match the experimental data. Rather, a systematic set of input guidelines for RGMX were used for all the HOVER rotor configurations. These guidelines were based on the method used in reference 20, where the selection of RGMX was directed by the calculations of the momentum analysis. Since this method did not result in good correlation with the experimental data, further work will be required to establish input guidelines for RGMX in the HOVER program.

As was mentioned earlier, these experimental data did not follow the performance trends shown in previous work (refs. 11 and 19). Since these rotor blades have less twist than the earlier configurations, the analytical methods were used to determine the effect of twist on the rotor hover performance. The results are shown in figure 8, where it can be seen that none of the analytical methods predicted significant changes in the rotor performance because of twist changes. These results are shown for the 75-percent tapered rotor; the results for the other configurations were similar. Since the analytical methods were not sensitive to large changes in twist, they could not be used to determine whether the differences between these data and previous data (refs. 11 and 19) were due to the effect of twist.

Summary of Results

A hover test was conducted on a small-scale model using three tapered rotor systems and a baseline rectangular-planform rotor system. The tapered-blade planforms had taper initiating at 50, 75, and 94 percent of the blade radius with a taper ratio of 3 to 1 for each blade set. The rotors had identical twist, airfoils, and thrust-weighted solidity. The blades were tested over a range of thrust coefficients, and the resulting data were compared with the predictions of three analytical methods. The analyses used were a simple momentum blade-element analysis and two free-wake, lifting-surface hover-performance analyses (HOVER and LSAF). The results of the investigation are summarized as follows:

1. The experimental data show that the 94-percent tapered rotor is slightly more efficient at the higher thrust coefficients than the other tapered configurations and the baseline rectangular rotor.
2. The other tapered-planform rotors did not show the expected improvement over the baseline rotor, and all configurations had a similar performance for low thrust coefficients.
3. The experimental data for the tapered configurations do not show a significant sensitivity to tip Reynolds number.
4. None of the three analytical methods used in this investigation showed good agreement with the experimental data, either in predicting the trend seen in the experimental data or in the level of performance that was measured.

NASA Langley Research Center
Hampton, VA 23665-5225
September 19, 1989

References

1. Tauber, Michael E.: Analytic Investigation of Advancing Blade Drag Reduction by Tip Modifications. *American Helicopter Society 34th Annual National Forum, 1978*, pp. 78-1-1–78-1-9.
2. Rabbott, John P., Jr.; and Neibanck, Charles: Experimental Effects of Tip Shape on Rotor Control Loads. *American Helicopter Society 34th Annual National Forum, 1978*, pp. 78-61-1–78-61-9.
3. Weller, William H.: *Experimental Investigation of Effects of Blade Tip Geometry on Loads and Performance for an Articulated Rotor System.* NASA TP-1303, AVRADCOM TR-78-53, 1979.

4. Stroub, Robert H.: *An Investigation of a Full-Scale Rotor With Four Blade Tip Planform Shapes.* NASA TM-78580, AVRADCOM TR-79-14, 1979.
5. Ballard, John D.; Orloff, Kenneth L.; and Luebs, Alan B.: Effect of Tip Shape on Blade Loading Characteristics for a Two-Bladed Rotor in Hover. *American Helicopter Society 35th Annual National Forum, 1979*, pp. 79-1-1–79-1-8.
6. Berry, John D.; and Mineck, Raymond E.: *Wind-Tunnel Test of an Articulated Helicopter Rotor Model With Several Tip Shapes.* NASA TM-80080, AVRADCOM TR-79-49, 1980.
7. Philippe, J. J.; and Vuillet, A.: Aerodynamic Design of Advanced Rotors With New Tip Shapes. *American Helicopter Society 39th Annual Forum, 1983*, pp. 58–71.
8. Balch, D. T.; and Lombardi, J.: *Experimental Study of Main Rotor Tip Geometry and Tail Rotor Interactions in Hover. Vol I—Text and Figures.* NASA CR-177336-Vol-I, 1985.
9. Desopper, A.; Lafon, P.; Ceroni, P.; and Philippe, J. J.: *10 Years of Rotor Flows Studies at ONERA—State of the Art and Future Studies.* ONERA T.P. No. 1986-49, June 1986.
10. Bingham, Gene J.: The Aerodynamic Influences of Rotor Blade Airfoils, Twist, Taper and Solidity on Hover and Forward Flight Performance. *Proceedings of the 37th Annual Forum, American Helicopter Soc., May 1981*, pp. 37–50.
11. Berry, John D.: *Performance Testing of a Main Rotor System for a Utility Helicopter at 1/4 Scale.* NASA TM-83274, AVRADCOM TR 82-B-3, 1982.
12. Kelley, H. L.; and Wilson, J. C.: Aerodynamic Performance of a 27-Percent-Scale AH-64 Wind-Tunnel Model With Baseline/Advanced Rotor Blades. *Proceedings of the 41st Annual Forum, American Helicopter Soc., May 1985*, pp. 491–499.
13. Yeager, William T., Jr.; Mantay, Wayne R.; Wilbur, Matthew L.; Cramer, Robert G., Jr.; and Singleton, Jeffrey D.: *Wind-Tunnel Evaluation of an Advanced Main-Rotor Blade Design for a Utility-Class Helicopter.* NASA TM-89129, AVSCOM TM 87-B-8, 1987.
14. Freeman, Carl E.; and Mineck, Raymond E.: *Fuselage Surface Pressure Measurements of a Helicopter Wind-Tunnel Model With a 3.15-Meter Diameter Single Rotor.* NASA TM-80051, 1979.
15. Phelps, Arthur E., III; and Berry, John D.: *Description of the U.S. Army Small-Scale 2-Meter Rotor Test System.* NASA TM-87762, AVSCOM TM 86-B-4, 1987.
16. Noonan, Kevin W.; and Bingham, Gene J.: *Aerodynamic Characteristics of Three Helicopter Rotor Airfoil Sections at Reynolds Numbers From Model Scale to Full Scale at Mach Numbers From 0.35 to 0.90.* NASA TP-1701, AVRADCOM TR 80-B-5, 1980.
17. Noonan, Kevin W.: *High Lift, Low Pitching Moment Airfoils.* U.S. Patent No. 4,776,531, Oct. 11, 1988.
18. *Instruments and Apparatus, Part 1—Measurement Uncertainty.* Supplement to ASME Performance Test Codes. ANSI/ASME PTC 19.1-1985, American Soc. of Mechanical Engineers, c.1986.
19. Phelps, Arthur E., III; and Althoff, Susan L.: *Effects of Planform Geometry on Hover Performance of a 2-Meter-Diameter Model of a Four-Bladed Rotor.* NASA TM-87607, AVSCOM TR 85-B-6, 1986.
20. Althoff, Susan L.: *Effect of Advanced Rotorcraft Airfoil Sections on the Hover Performance of a Small-Scale Rotor Model.* NASA TP-2832, AVSCOM TP-88-B-001, 1988.
21. Gessow, Alfred; and Myers, Garry C., Jr.: *Aerodynamics of the Helicopter.* College Park Press, c.1952.
22. Summa, J. Michael: Advanced Rotor Analysis Methods for the Aerodynamics of Vortex/Blade Interactions in Hover. *Eighth European Rotorcraft and Powered Lift Aircraft Forum* (Aix-en-Province, France), Aug.–Sept. 1982, Paper No. 2.8.
23. Kocurek, J. David; and Berkowitz, Leonard F.: Velocity Coupling—A New Concept for Hover and Axial Flow Wake Analysis and Design. *Prediction of Aerodynamic Loads on Rotorcraft*, AGARD-CPP-334, Apr. 1982, pp. 8-1–8-13.
24. Kocurek, J. David; and Tangler, James L.: A Prescribed Wake Lifting Surface Hover Performance Analysis. *J. American Helicopter Soc.*, vol. 22, no. 1, Jan. 1977, pp. 24–35.
25. Bellinger, E. Dean: *Experimental Investigation of Effects of Blade Section Camber and Planform Taper on Rotor Hover Performance.* USAAMRDL TR-72-4, U.S. Army, Mar. 1972.

Table I. Airfoil Coordinates for RC(4)-10

[Stations and ordinates given in fraction of airfoil chord]

Station	Lower surface
1.000000	0.000203
.975148	−.003160
.950227	−.005728
.925298	−.008079
.900374	−.010312
.875421	−.012443
.850386	−.014420
.825282	−.016215
.800114	−.017818
.774866	−.019273
.749797	−.020610
.724840	−.021873
.699792	−.023108
.674849	−.024327
.649997	−.025542
.625136	−.026750
.600297	−.027933
.575437	−.029062
.550567	−.030090
.525714	−.030972
.500894	−.031659
.476002	−.032163
.451451	−.032474
.426974	−.032600
.402303	−.032553
.377696	−.032369
.352929	−.032090
.303398	−.031393
.254059	−.030703
.229490	−.030430
.204930	−.030257
.180495	−.030276
.156116	−.030611
.132051	−.031269
.108242	−.032011
.084979	−.032337
.061865	−.031576
.035595	−.028199
.025184	−.025664
.016462	−.022703
.014350	−.021823
.004687	−.015907

Station	Upper surface
0.000000	−0.005726
.002864	.004313
.009072	.013175
.023543	.025980
.047036	.038875
.073686	.047953
.100188	.053673
.126143	.057324
.151842	.059790
.177227	.061579
.202556	.062995
.227760	.064163
.252956	.065143
.303145	.066614
.353142	.067381
.378140	.067422
.403297	.067163
.428390	.066543
.453678	.065499
.478891	.064013
.503763	.062129
.528707	.059876
.553618	.057324
.578512	.054510
.603417	.051447
.628341	.048144
.653244	.044621
.678157	.040912
.702978	.037093
.727694	.033251
.752502	.029451
.777197	.025808
.801713	.022378
.826309	.019139
.850970	.016086
.875699	.013211
.900509	.010514
.925350	.008012
.950185	.005722
.975028	.003652
1.000000	.001785

Table II. Airfoil Coordinates for RC(3)-10

[Stations and ordinates given in fraction of airfoil chord]

Station	Lower surface
1.00000	−0.00020
.96828	−.00633
.93631	−.01171
.90409	−.01594
.87082	−.01959
.83623	−.02272
.80002	−.02536
.76185	−.02758
.72232	−.02939
.68276	−.03079
.64378	−.03184
.60547	−.03260
.56746	−.03313
.52949	−.03346
.49148	−.03360
.45336	−.03357
.41524	−.03337
.37733	−.03301
.33995	−.03249
.30343	−.03184
.26807	−.03107
.23402	−.03020
.20137	−.02923
.17023	−.02817
.14075	−.02696
.11305	−.02561
.08724	−.02400
.06347	−.02203
.04214	−.01950
.02403	−.01619
.01090	−.01230
.00310	−.00765

Station	Upper surface
0.00000	0.00000
.00310	.00906
.01090	.01700
.02403	.02462
.04214	.03193
.06347	.03854
.08724	.04435
.11305	.04944
.14075	.05376
.17023	.05748
.20137	.06051
.23402	.06292
.26807	.06474
.30343	.06596
.33995	.06661
.37733	.06672
.41524	.06627
.45336	.06528
.49148	.06376
.52949	.06170
.56746	.05909
.60547	.05593
.64378	.05220
.68276	.04787
.72232	.04296
.76185	.03758
.80002	.03200
.83623	.02644
.87082	.02096
.90409	.01564
.93631	.01052
.96828	.00600
1.00000	.00180

Table III. Airfoil Coordinates for RC(3)-08

[Stations and ordinates given in fraction of airfoil chord]

Station	Lower surface
1.00000	−0.00050
.96782	−.00513
.93543	−.00942
.90280	−.01293
.86927	−.01599
.83457	−.01867
.79842	−.02099
.76057	−.02300
.72150	−.02469
.68238	−.02605
.64367	−.02713
.60553	−.02796
.56766	−.02858
.52983	−.02902
.49199	−.02929
.45404	−.02939
.41612	−.02934
.37840	−.02913
.34121	−.02877
.30484	−.02853
.26959	−.02791
.23560	−.02693
.20298	−.02609
.17186	−.02513
.14239	−.02403
.11471	−.02278
.08889	−.02129
.06508	−.01951
.04369	−.01729
.02534	−.01445
.01170	−.01096
.00314	−.00656

Station	Upper surface
0.00000	0.00000
.00314	.00671
.01170	.01312
.02534	.01900
.04369	.02455
.06508	.02952
.08889	.03389
.11471	.03770
.14239	.04096
.17186	.04376
.20298	.04606
.23560	.04789
.26959	.04928
.30484	.05023
.34121	.05075
.37840	.05087
.41612	.05057
.45404	.04986
.49199	.04876
.52983	.04725
.56766	.04533
.60553	.04300
.64367	.04024
.68238	.03704
.72150	.03342
.76057	.02944
.79842	.02528
.83457	.02107
.86927	.01686
.90280	.01271
.93543	.00864
.96782	.00490
1.00000	.00130

Table IV. Experimental Data for Rectangular-Planform Rotor

C_T	FM	C_Q
0.00192	0.320	0.000186
.00199	.337	.000187
.00259	.429	.000217
.00270	.453	.000219
.00333	.520	.000261
.00410	.571	.000325
.00417	.587	.000324
.00497	.633	.000391
.00501	.637	.000393
.00510	.643	.000401
.00614	.672	.000506
.00618	.688	.000499
.00656	.682	.000551
.00671	.688	.000564
.00721	.699	.000619
.00726	.704	.000621
.00780	.701	.000694
.00798	.715	.000704
.00834	.701	.000767
.00839	.716	.000759
.00880	.714	.000816
.01058	.720	.001067

Table V. Experimental Data for 94-Percent Tapered Rotor

C_T	FM	C_Q
0.00227	0.367	0.000208
.00232	.375	.000210
.00235	.383	.000210
.00295	.464	.000244
.00302	.477	.000246
.00304	.489	.000242
.00374	.554	.000292
.00387	.569	.000299
.00390	.588	.000292
.00467	.635	.000355
.00468	.633	.000357
.00487	.643	.000374
.00511	.666	.000388
.00569	.679	.000446
.00570	.690	.000440
.00588	.692	.000461
.00618	.681	.000504
.00623	.695	.000500
.00630	.706	.000501
.00668	.707	.000546
.00676	.705	.000557
.00686	.724	.000554
.00733	.720	.000615
.00794	.744	.000672
.00801	.733	.000691
.00848	.728	.000757
.00850	.737	.000751
.00907	.720	.000848
.00915	.725	.000854

Table VI. Experimental Data for 75-Percent Tapered Rotor

C_T	FM	C_Q
0.00114	0.176	0.000155
.00169	.274	.000180
.00170	.276	.000178
.00174	.293	.000175
.00236	.395	.000205
.00244	.411	.000207
.00254	.438	.000206
.00307	.470	.000255
.00312	.496	.000249
.00320	.503	.000254
.00384	.547	.000308
.00385	.561	.000301
.00386	.547	.000310
.00435	.582	.000348
.00446	.608	.000345
.00478	.628	.000371
.00479	.617	.000380
.00481	.619	.000381
.00518	.647	.000407
.00531	.648	.000422
.00578	.672	.000463
.00579	.670	.000464
.00582	.656	.000478
.00629	.686	.000513
.00629	.682	.000517
.00682	.696	.000572
.00682	.696	.000572
.00682	.681	.000585
.00731	.694	.000636
.00737	.696	.000642
.00768	.695	.000685
.00782	.708	.000691
.00818	.702	.000744
.00825	.705	.000751
.00867	.699	.000817
.00869	.697	.000820
.00871	.700	.000820
.00906	.697	.000875
.00919	.686	.000908
.00919	.685	.000908
.00960	.675	.000985
.00967	.674	.000995

Table VII. Experimental Data for 50-Percent Tapered Rotor

C_T	FM	C_Q
0.00198	0.328	0.000189
.00200	.328	.000192
.00208	.345	.000193
.00265	.422	.000228
.00267	.438	.000223
.00269	.434	.000227
.00343	.517	.000274
.00349	.516	.000282
.00362	.542	.000283
.00432	.589	.000340
.00433	.598	.000337
.00441	.595	.000348
.00517	.635	.000413
.00535	.657	.000421
.00535	.648	.000427
.00573	.661	.000464
.00621	.690	.000501
.00635	.692	.000517
.00637	.693	.000518
.00679	.707	.000559
.00689	.703	.000574
.00726	.716	.000611
.00734	.704	.000631
.00737	.704	.000635
.00789	.716	.000691
.00792	.708	.000704
.00842	.719	.000759
.00846	.710	.000774
.00882	.700	.000836
.00891	.716	.000830
.00928	.682	.000927

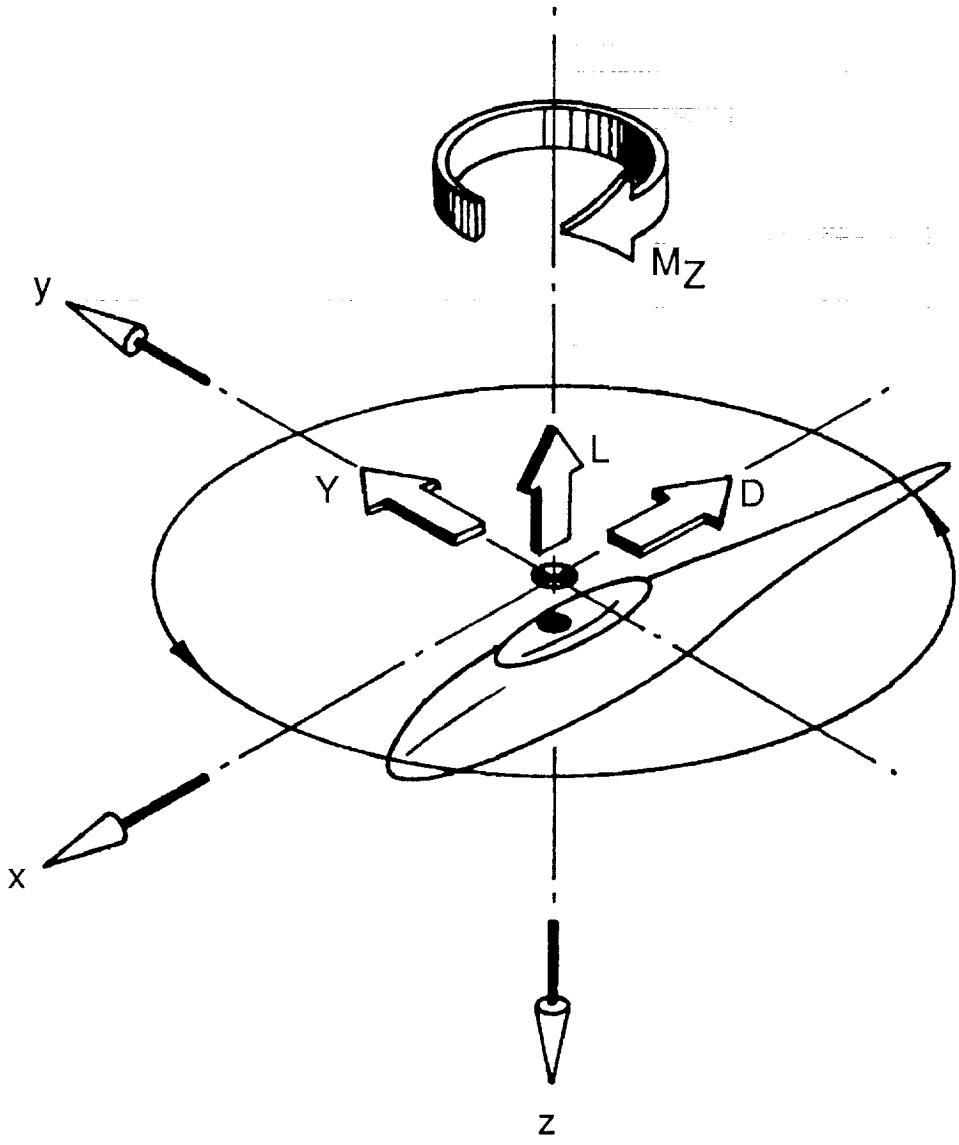

Figure 1. Axis system used for presentation of data. Arrows denote positive directions of forces, moments, and axes.

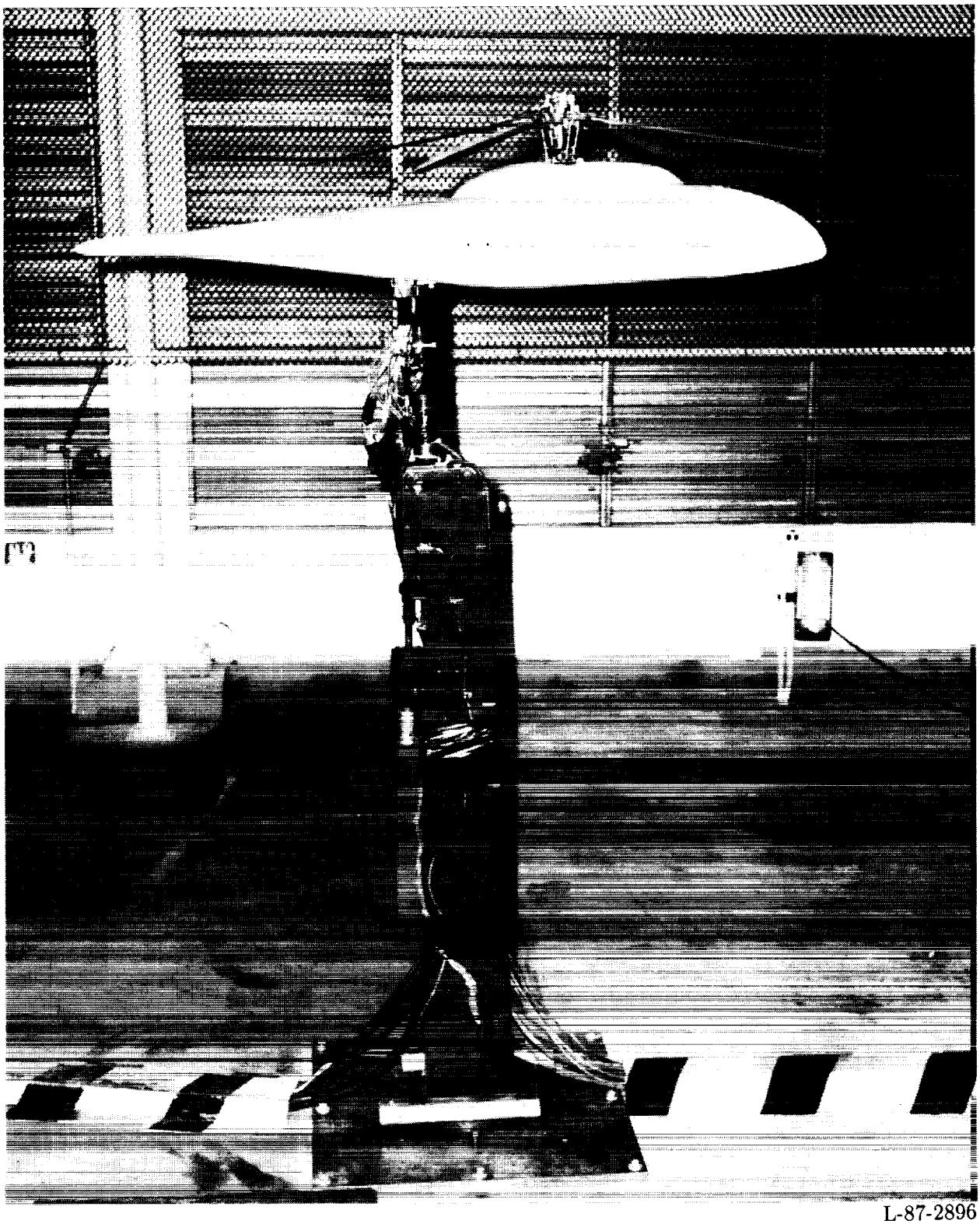

(a) Model mounted for testing.

Figure 2. Photograph of test configuration in rotor test cell.

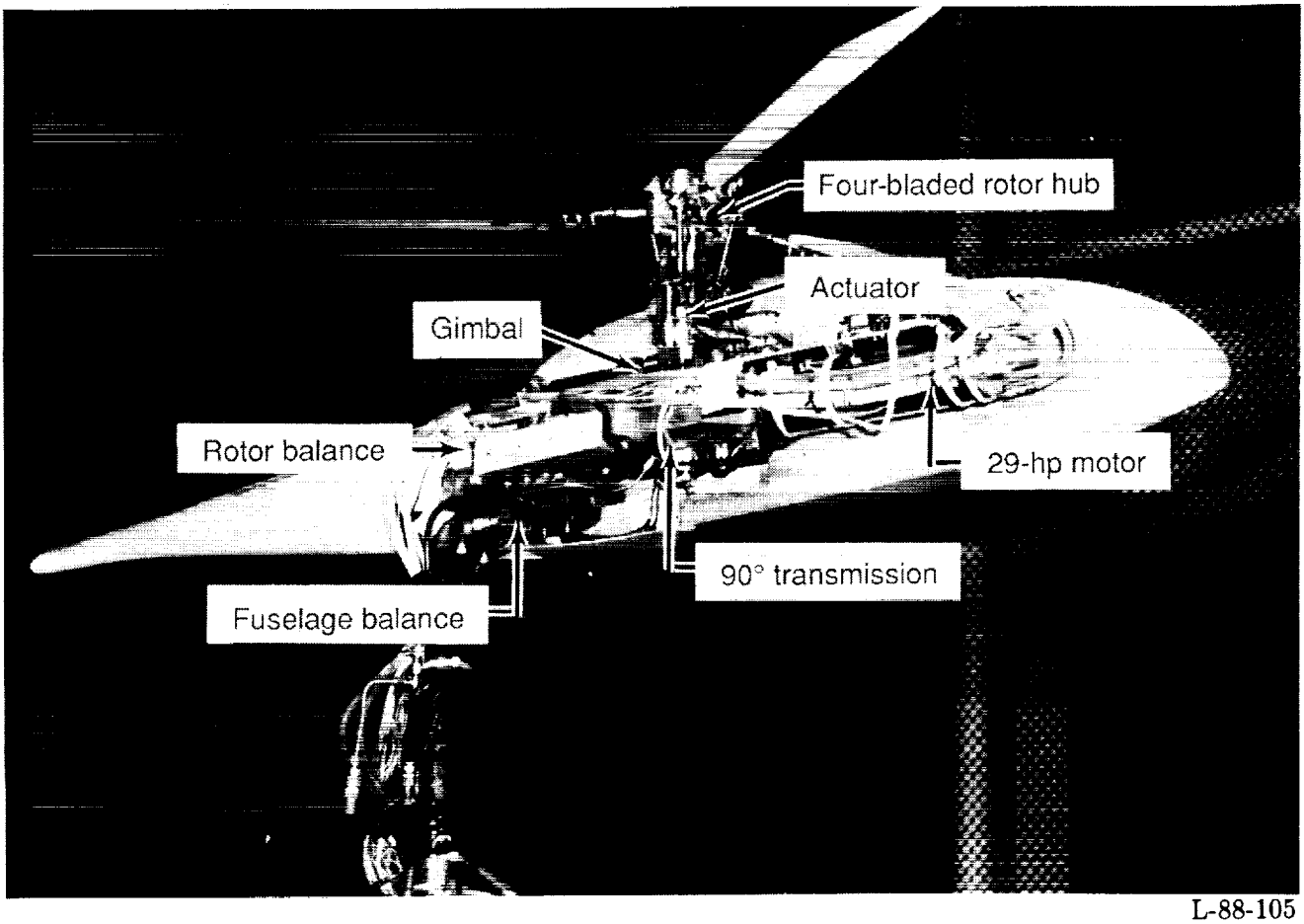

L-88-105

(b) Cutaway view of 2MRTS.

Figure 2. Concluded.

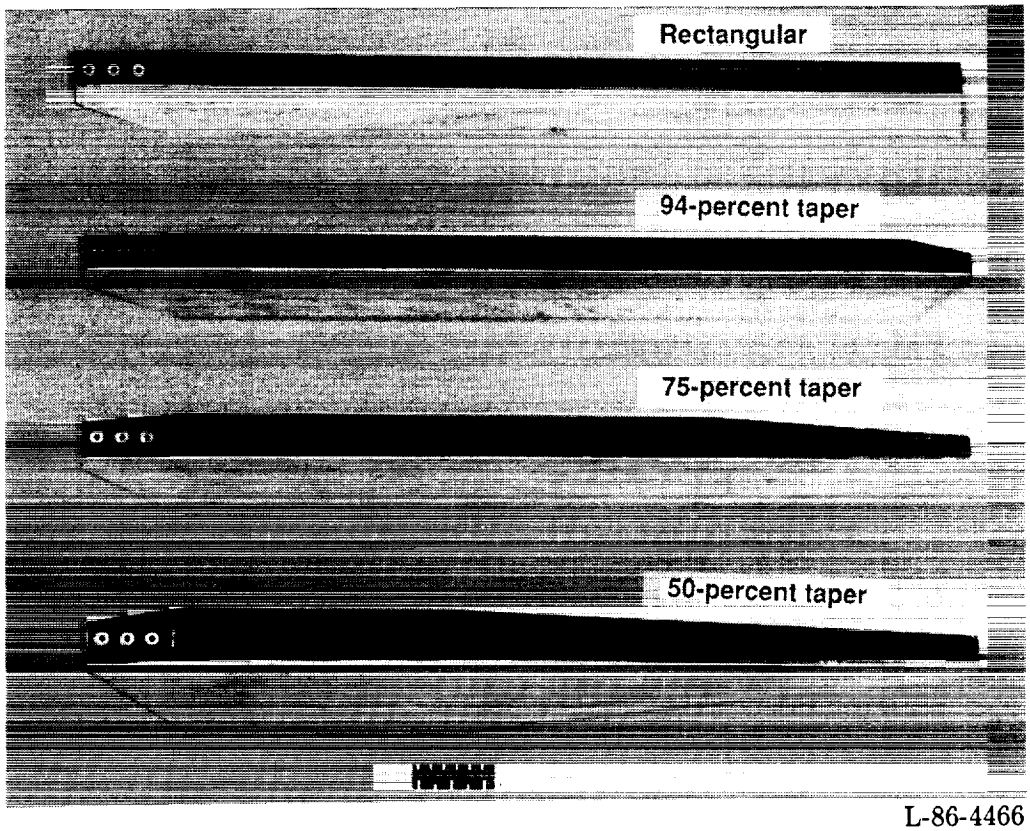

L-86-4466

(a) Photograph of four blade planforms.

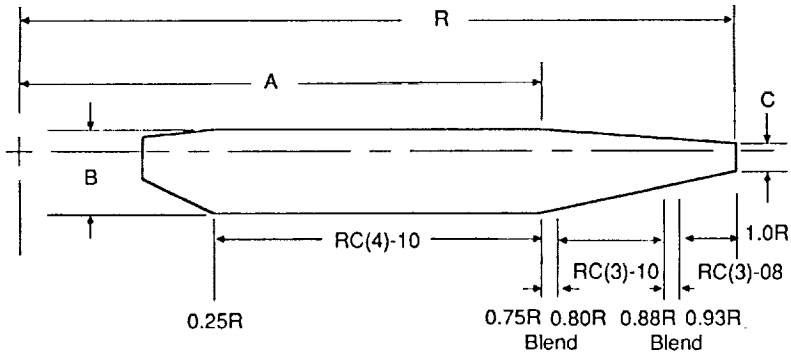

Blade	Twist, deg	R, ft	A	B	C
Rectangular	-13	2.708	1.00R	0.0770R	0.0770R
94% Taper	-13	2.708	0.94R	0.0817R	0.0272R
75% Taper	-13	2.708	0.75R	0.0972R	0.0324R
50% Taper	-13	2.708	0.50R	0.1194R	0.0398R

(b) Description of planform and airfoil distribution.

Figure 3. Description of rotor blades.

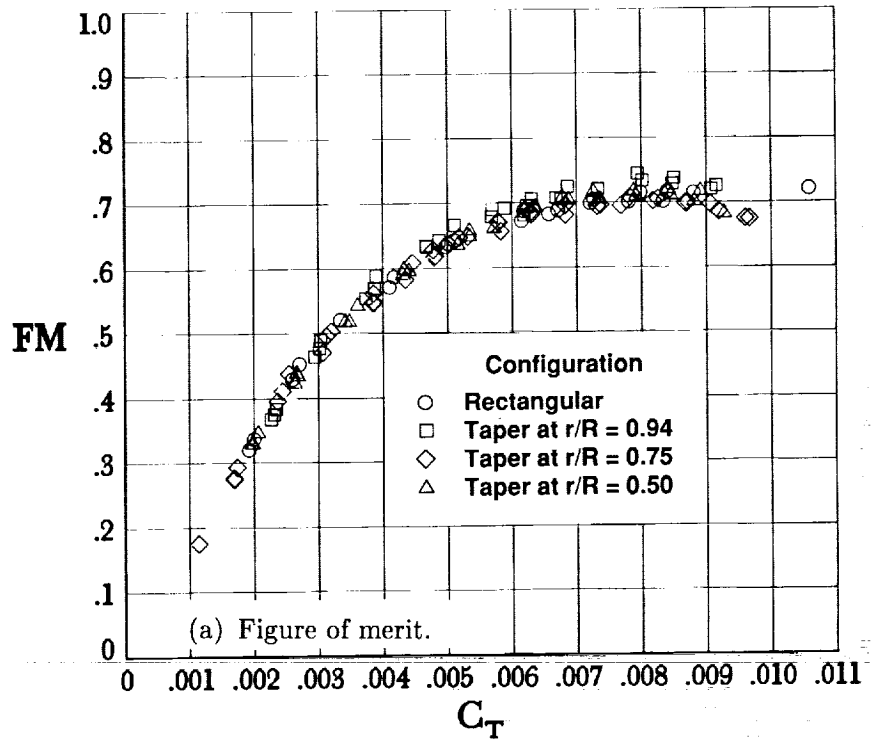

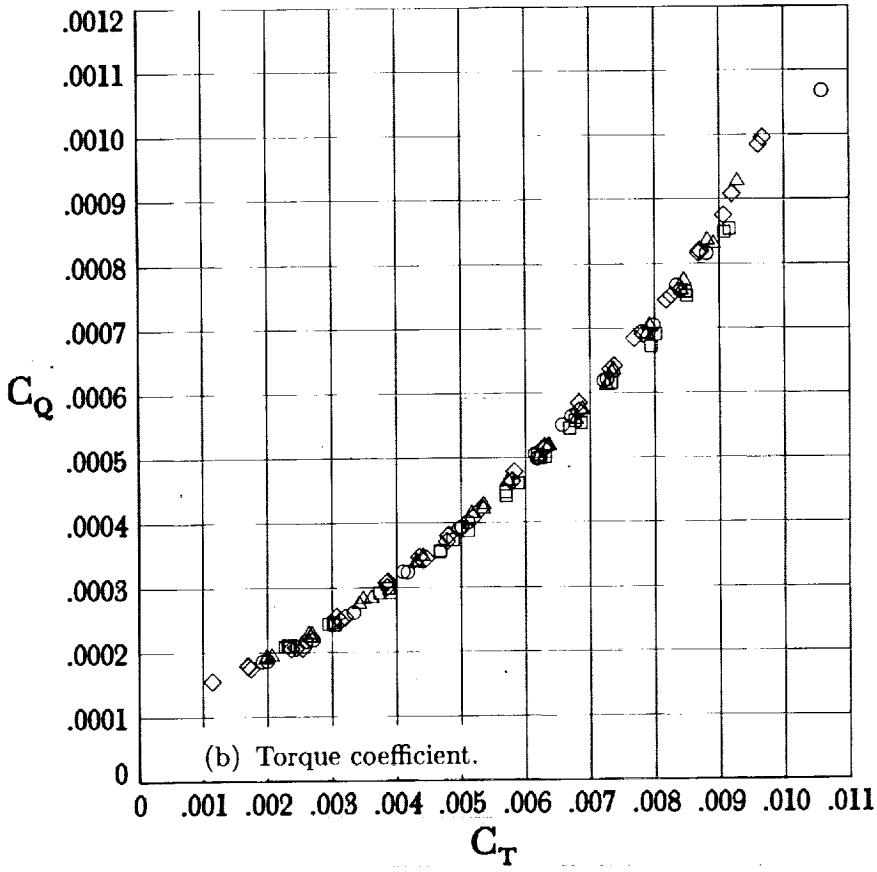

Figure 4. Comparison of basic aerodynamic characteristics of rotors.

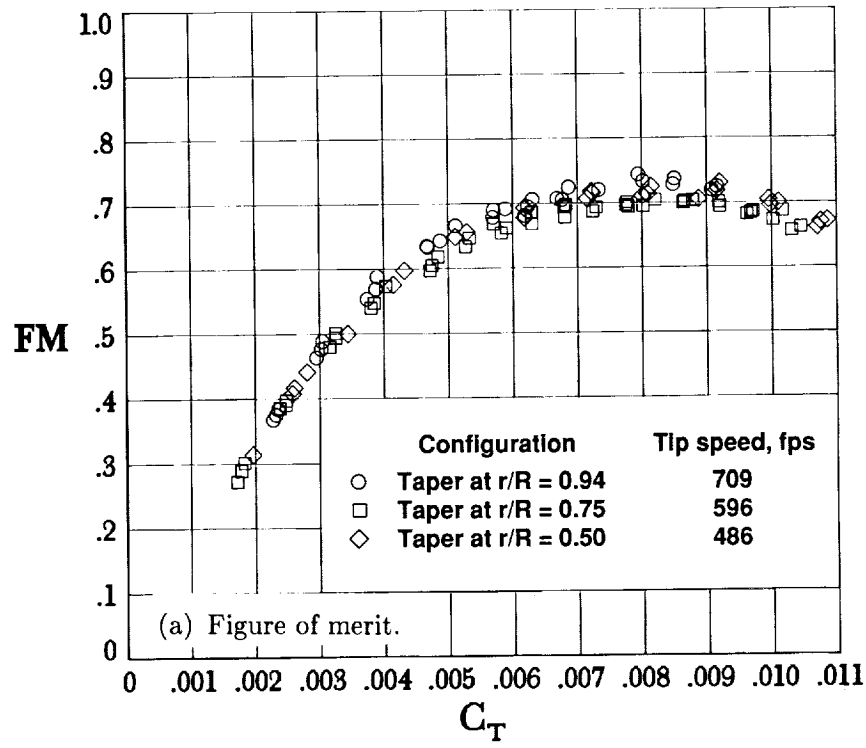

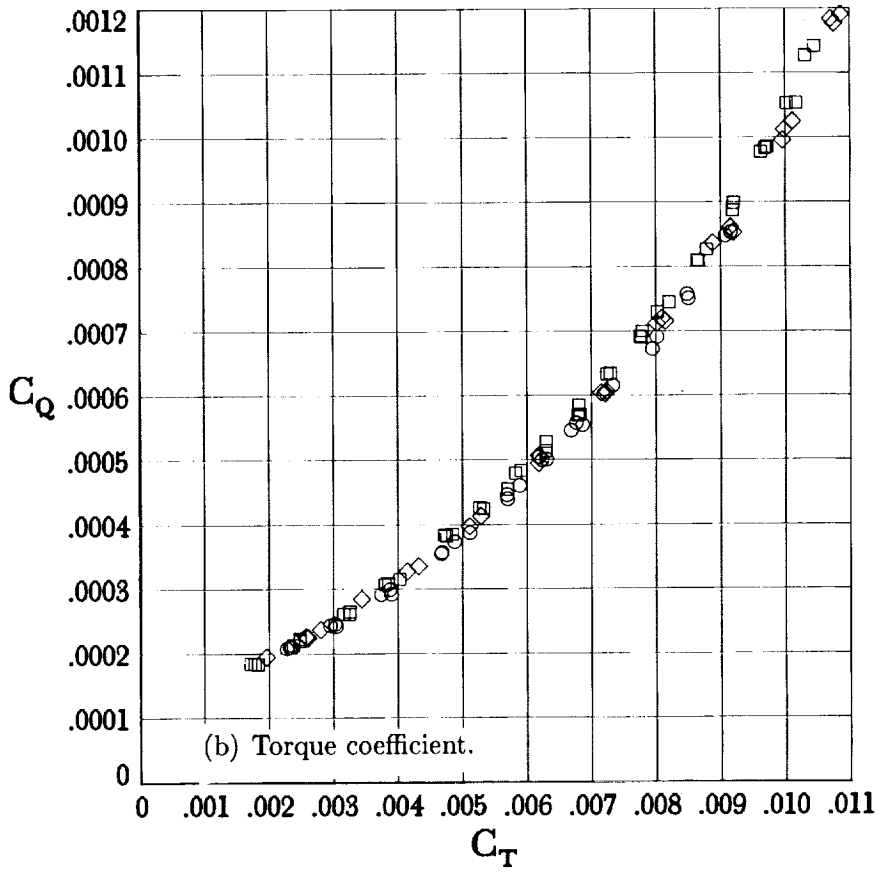

Figure 5. Comparison of tapered rotors at a tip Reynolds number of 332 562.

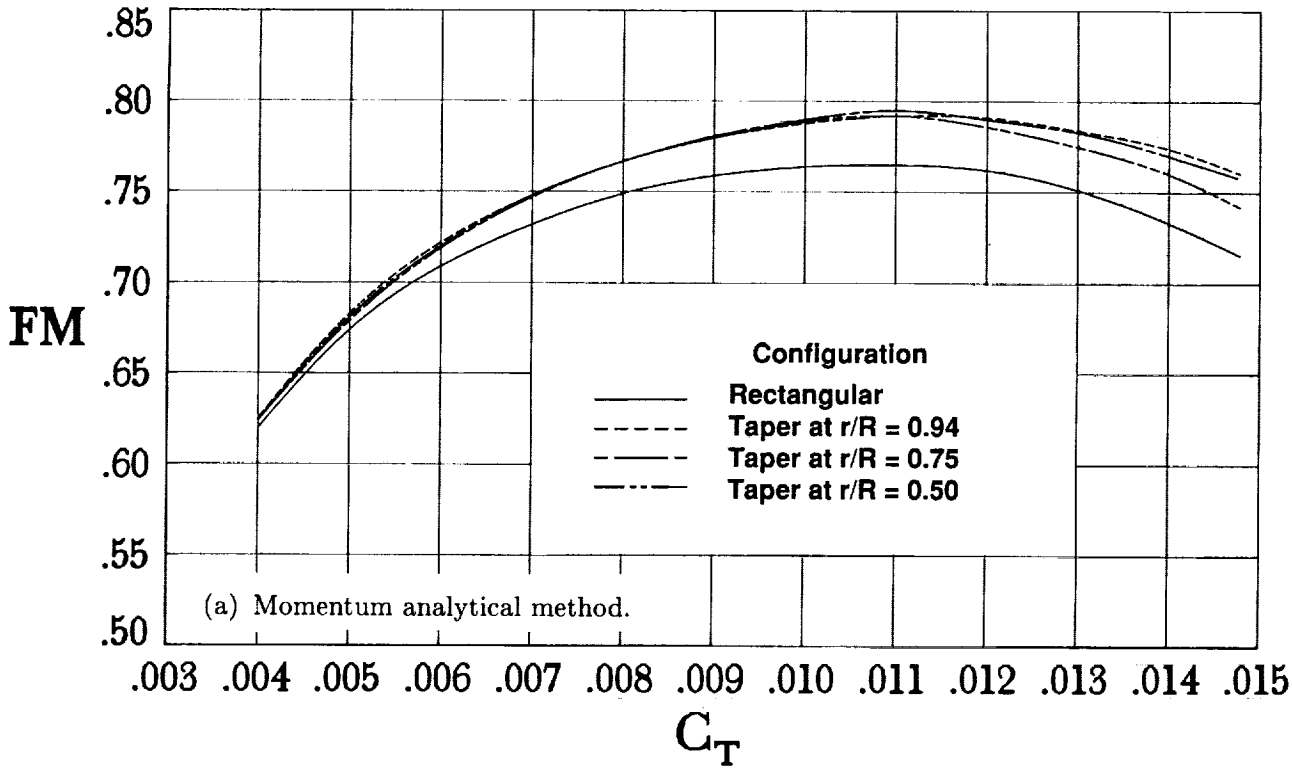

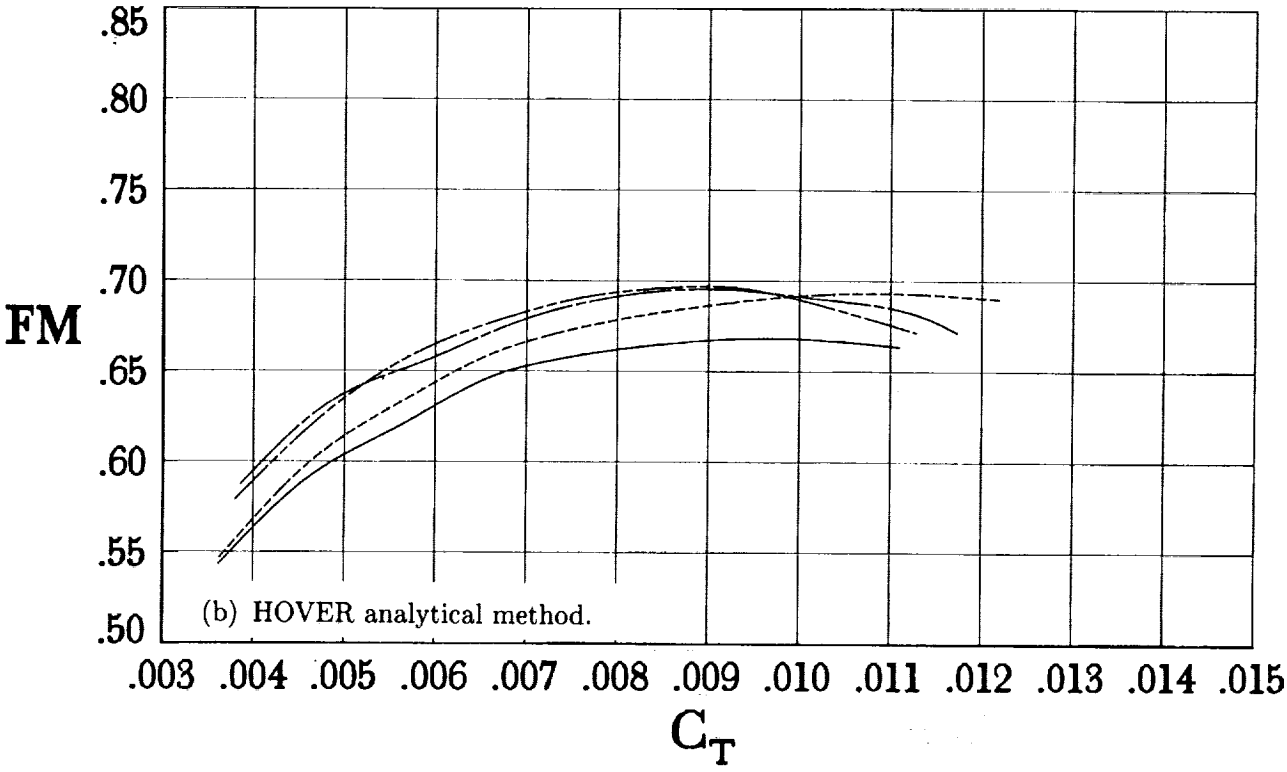

Figure 6. Comparison of trends predicted by analyses.

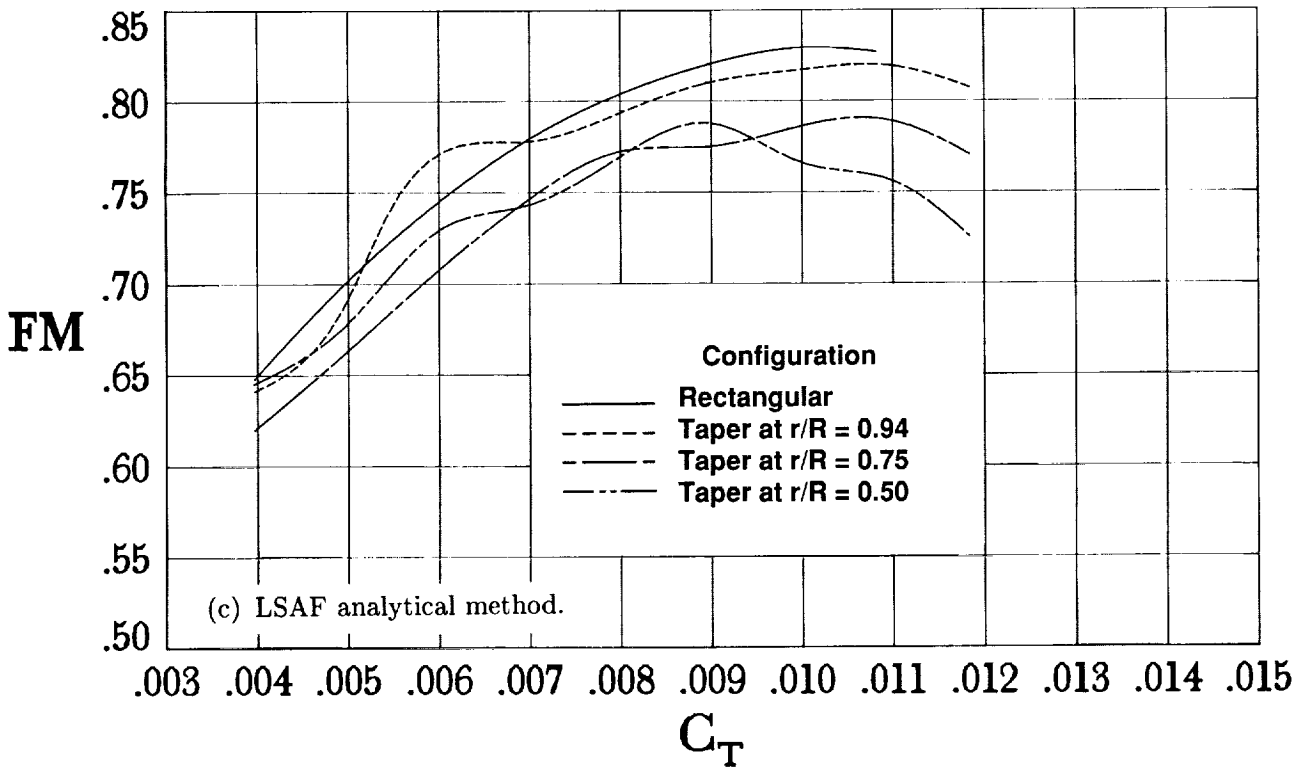

Figure 6. Concluded.

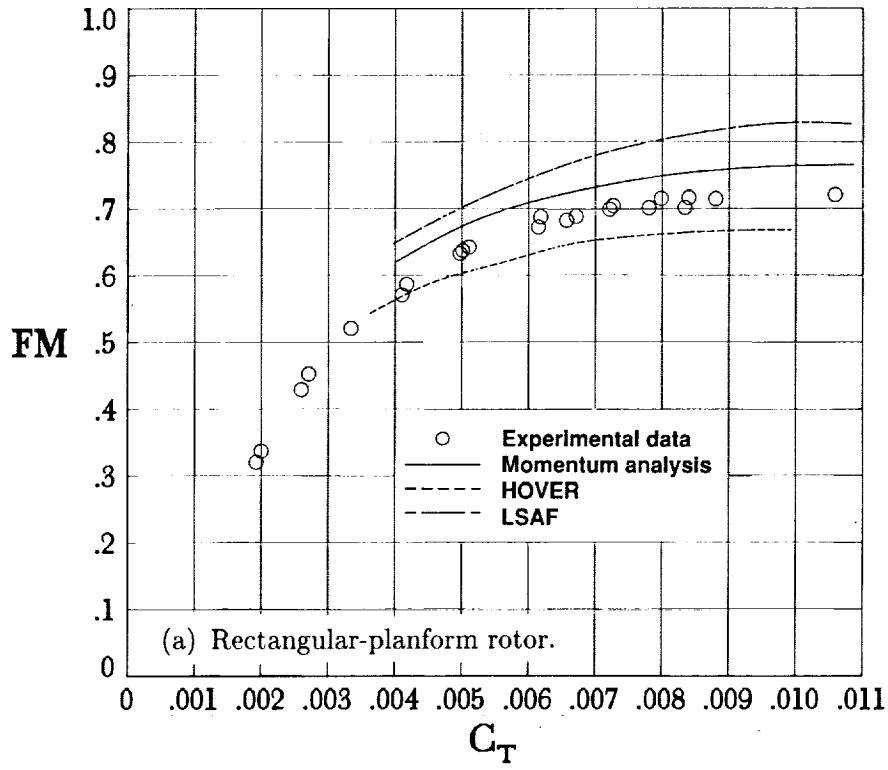

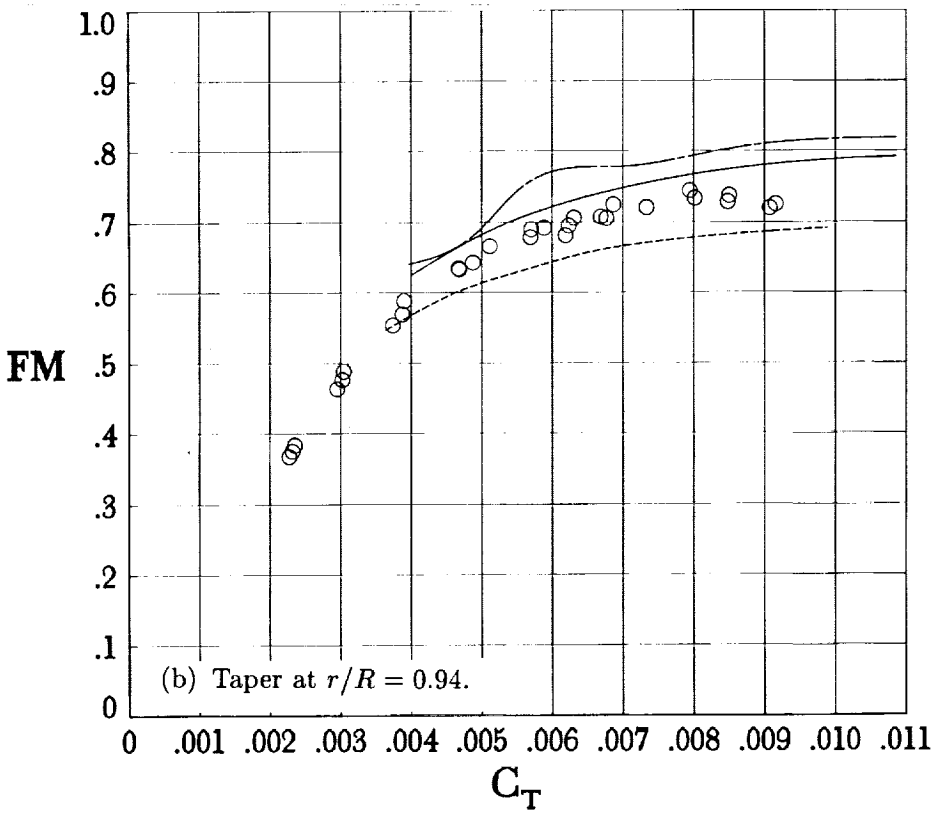

Figure 7. Comparison of prediction methods with experimental data.

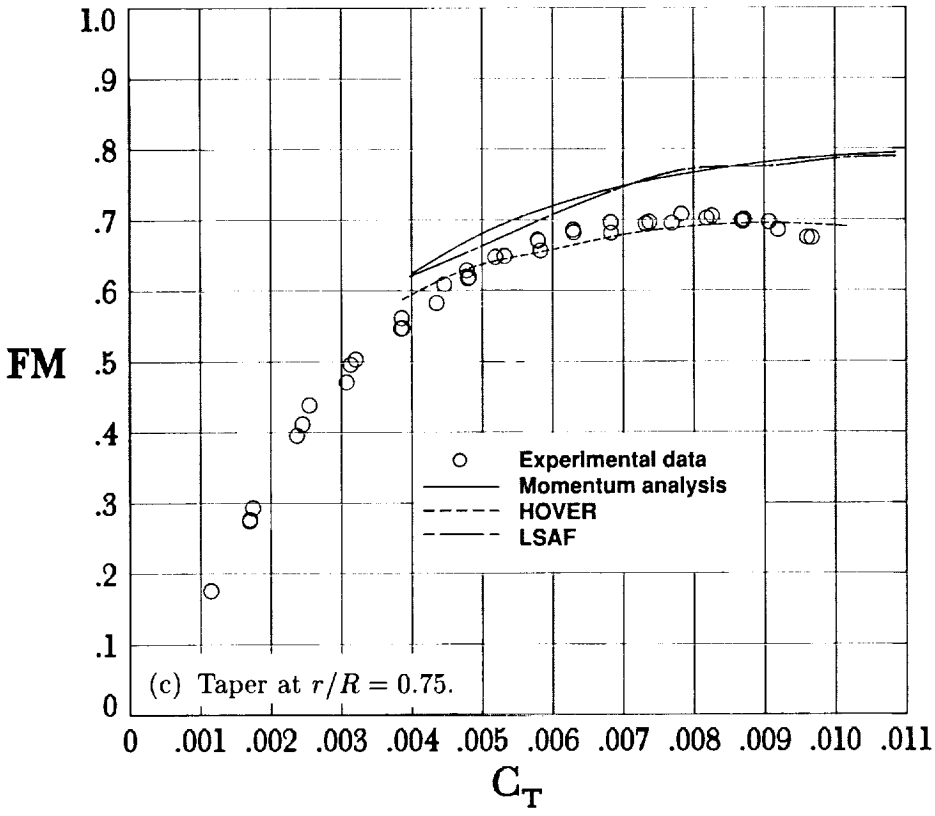

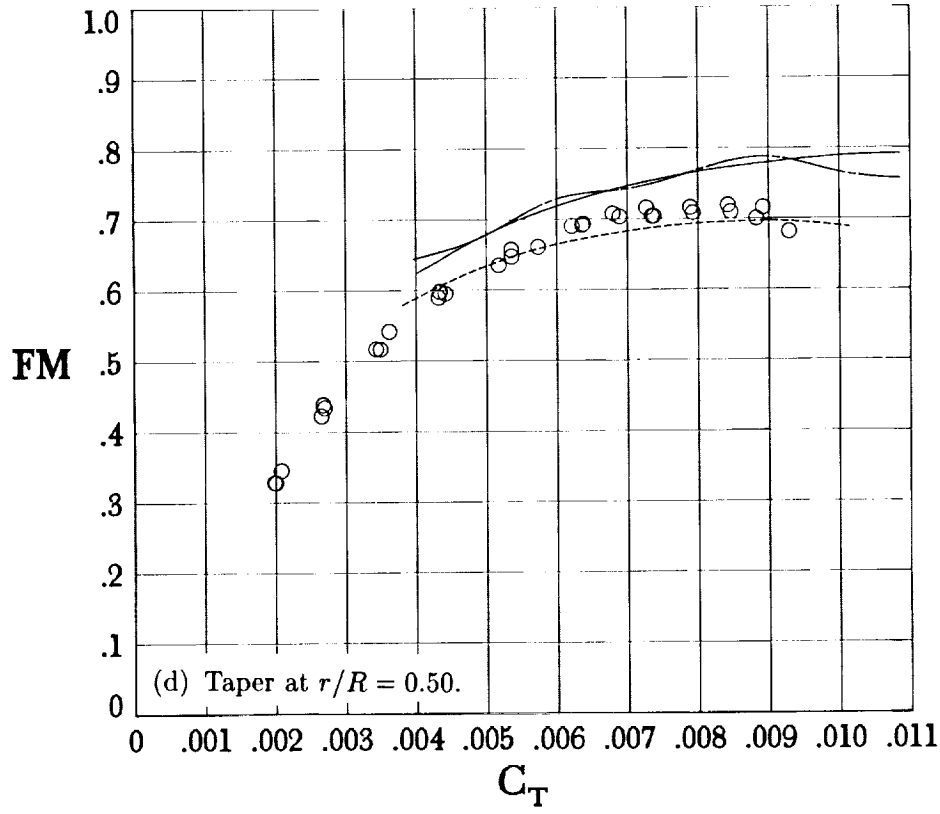

Figure 7. Concluded.

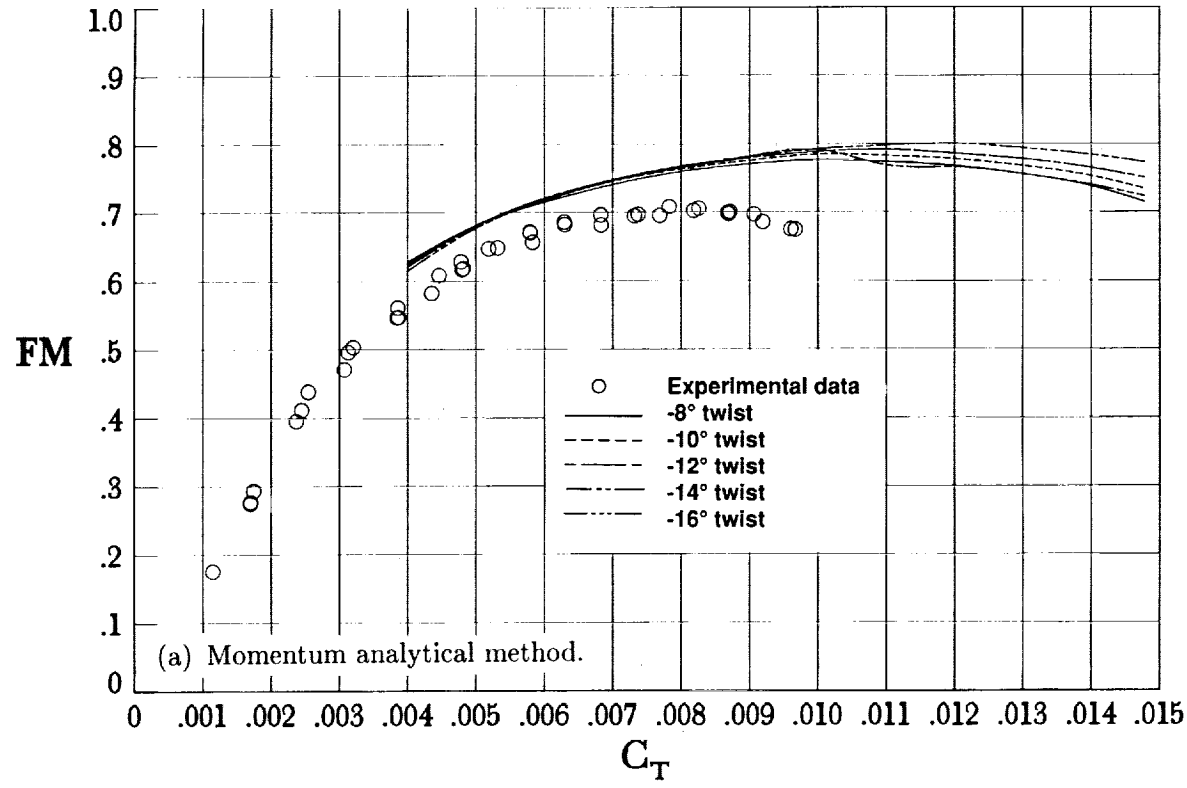

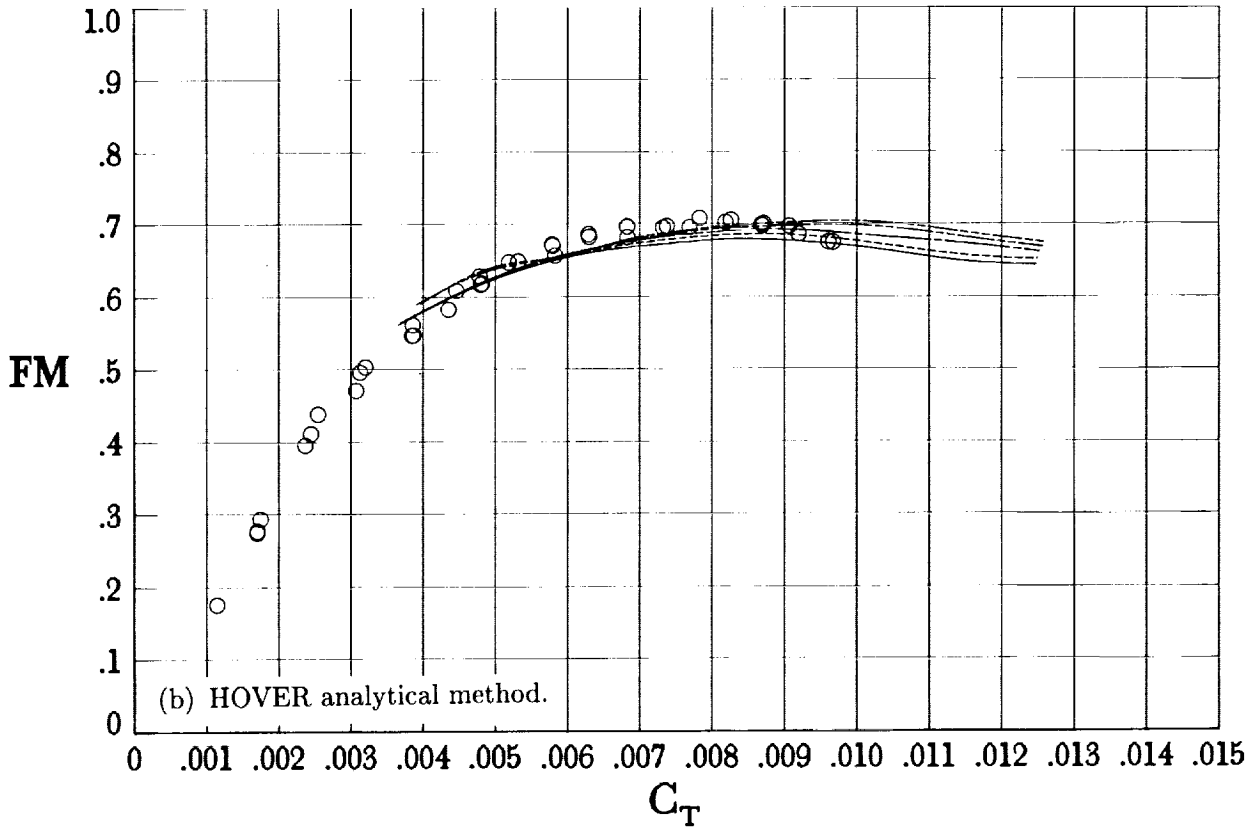

Figure 8. Comparison of prediction methods for several values of twist for taper at $r/R = 0.75$.

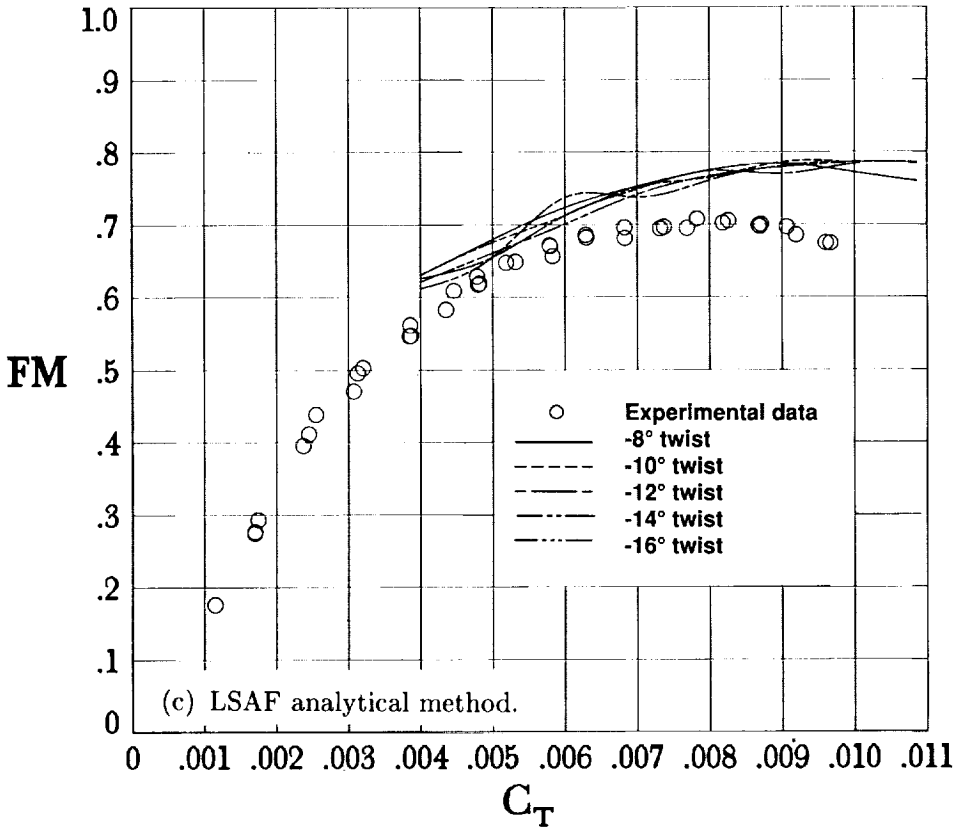

Figure 8. Concluded.

NASA
National Aeronautics and Space Administration

Report Documentation Page

1. Report No.	2. Government Accession No.	3. Recipient's Catalog No.
NASA TM-4146 AVSCOM TM-89-B009		

4. Title and Subtitle	5. Report Date
Effect of Blade Planform Variation on a Small-Scale Hovering Rotor	January 1990
	6. Performing Organization Code
7. Author(s)	8. Performing Organization Report No.
Susan L. Althoff and Kevin W. Noonan	L-16608
9. Performing Organization Name and Address	10. Work Unit No.
Aerostructures Directorate USAARTA-AVSCOM Langley Research Center Hampton, VA 23665-5225	505-61-51-10
	11. Contract or Grant No.
12. Sponsoring Agency Name and Address	13. Type of Report and Period Covered
National Aeronautics and Space Administration Washington, DC 20546-0001 and U.S. Army Aviation Systems Command St. Louis, MO 63120-1798	Technical Memorandum
	14. Army Project No.
	1L161102AH45A

15. Supplementary Notes

Susan L. Althoff and Kevin W. Noonan: Aerostructures Directorate, USAARTA-AVSCOM, Hampton, Virginia.

16. Abstract

A hover test was conducted on a small-scale rotor model for three sets of tapered rotor blades and a baseline rectangular-planform rotor blade. All configurations had the same airfoils, twist, and thrust-weighted solidity. The tapered-blade planforms had taper initiating at 50, 75, and 94 percent of the blade radius with a taper ratio of 3 to 1 for each blade set. The experiment was conducted for a range of thrust coefficients, and the data were compared with the predictions of three hover analytical methods. The data show that the 94-percent tapered blade was slightly more efficient at the higher rotor thrust levels. The other tapered-planform rotors did not show the expected improvement over the baseline rotor, and all configurations had a similar performance for low thrust coefficients. None of the analytical methods correlated well with the experimental data.

17. Key Words (Suggested by Authors(s))	18. Distribution Statement
Rotor Hover Blade planform Taper Helicopter	Unclassified—Unlimited Subject Category 02

19. Security Classif. (of this report)	20. Security Classif. (of this page)	21. No. of Pages	22. Price
Unclassified	Unclassified	24	A03

NASA-Langley, 1990

NASA FORM 1626 OCT 86

For sale by the National Technical Information Service, Springfield, Virginia 22161-2171